

Numerical Stability Improvements for the Pseudo-Spectral EM PIC Algorithm

Brendan B. Godfrey,^{*}Jean-Luc Vay,[†]and Irving Haber[‡]

January 16, 2021

Abstract

The pseudo-spectral analytical time-domain (PSATD) particle-in-cell (PIC) algorithm solves the vacuum Maxwell's equations exactly, has no Courant time-step limit (as conventionally defined), and offers substantial flexibility in plasma and particle beam simulations. It is, however, not free of the usual numerical instabilities, including the numerical Cherenkov instability, when applied to relativistic beam simulations. This paper presents several approaches that, when combined with digital filtering, almost completely eliminate the numerical Cherenkov instability. The paper also investigates the numerical stability of the PSATD algorithm at low beam energies.

1 Introduction

The Pseudo Spectral Analytical Time Domain (PSATD) particle-in-cell (PIC) algorithm solves Maxwell's equations in spatial Fourier space, using equations that are exact for any time step, when the plasma current is constant [1]. Consequently, it has no Courant limit in the usual sense and, when combined with the Esirkepov conserved current algorithm [2], is highly accurate for relativistic

beam simulations. The PSATD algorithm nonetheless has received little attention over the past two decades, perhaps due to the belief that it could not be used efficiently on modern parallel computers. Recently, however, an approach to PSATD parallelization has been developed, and simulations performed to demonstrate its effectiveness [3].

The numerical stability properties of the PSATD-Esirkepov algorithm have been analyzed to develop methods of suppressing the all too pervasive numerical Cherenkov instability [4]. Results included a complete multidimensional numerical dispersion relation for cold relativistic beams, approximate analytical expressions for numerical instability peak growth rates, and numerical solutions of the dispersion relation for various choices of numerical parameters [5]. Importantly, this analysis demonstrated that numerical Cherenkov instability growth rates could be reduced by as much as two orders of magnitude by suitable choices of algorithm options and digital filtering.

In this paper still other approaches for suppressing the numerical Cherenkov instability are introduced. These new options require less digital filtering than before, preserving a larger portion of k-space for physical phenomena. Additionally, analysis of the numerical Cherenkov instability is extended to lower energies, where it eventually gives way to the well known electrostatic numerical instability [6, 7] for non-relativistic beams. An instability unique to pseudo-spectral algorithms, first predicted in [8], also is discussed.

^{*}Brendan Godfrey is with the University of Maryland, College Park, Maryland 20742, USA, e-mail: bren-dan.godfrey@ieee.org.

[†]Jean-Luc Vay is with Lawrence Berkeley National Laboratory, Berkeley, California 94720, USA, e-mail: jlvay@lbl.gov.

[‡]Irving Haber is with the University of Maryland, College Park, Maryland 20742, USA, e-mail: haber@umd.edu.

2 Prior Stability Results

Although multiple representations of the PSATD algorithm exist, the following is both compact and convenient for numerical analysis:

$$\mathbf{E}^{n+1} = \mathbf{E}^n - 2iS_h \mathbf{k} \times \mathbf{B}^{n+1/2}/k - S\zeta : \mathbf{J}_e^{n+1/2}/k + S\mathbf{k}\mathbf{k} \cdot \zeta : \mathbf{J}_e^{n+1/2}/k^3 - \mathbf{k}\mathbf{k} \cdot \mathbf{J}_e^{n+1/2} \Delta t/k^2, \quad (1)$$

$$\mathbf{B}^{n+3/2} = \mathbf{B}^{n+1/2} + 2iS_h \mathbf{k} \times \mathbf{E}^{n+1}/k, \quad (2)$$

with \mathbf{B}^n , needed to advance the particles, given by

$$\mathbf{B}^n = \frac{1}{2C_h} \left(\mathbf{B}^{n+1/2} + \mathbf{B}^{n-1/2} \right). \quad (3)$$

Quantities introduced in these and subsequent equations are given in [5], upon which this section of the paper is based.

Lengthy algebra, validated with Mathematica [9], leads to a dispersion relation of the form,

$$C_0 + n \sum_{m_z} C_1 \csc \left[(\omega - k'_z v) \frac{\Delta t}{2} \right] + n \sum_{m_z} (C_{2x} + \gamma^{-2} C_{2z}) \csc^2 \left[(\omega - k'_z v) \frac{\Delta t}{2} \right] + \gamma^{-2} n^2 \left(\sum_{m_z} C_{3z} \csc^2 \left[(\omega - k'_z v) \frac{\Delta t}{2} \right] \right) \left(\sum_{m_z} C_{3x} \csc \left[(\omega - k'_z v) \frac{\Delta t}{2} \right] \right) = 0, \quad (4)$$

with $k'_z = k_z + m_z 2\pi/\Delta z$ and m_z an integer. The factors, $\csc \left[(\omega - k'_z v) \frac{\Delta t}{2} \right]$, except that multiplying C_{3z} , are numerical artifacts. Coupling of the resulting numerical modes, $\omega = k'_z v$, with electromagnetic modes, $C_0 = 0$, causes the numerical Cherenkov instability.

The strategy used in [5] to suppress the relativistic beam simulation numerical Cherenkov instabilities is as follows. The fastest growing instabilities occur where the $m_z = 0, -1$ alias modes intersect the light cone, typically at large k , where they can be eliminated by digital filtering. The higher order aliases often are unstable at small k , but have small

growth rates that can be reduced even further by using higher order interpolation, say, cubic. Finally, the $m_z = 0, -1$ aliases often are unstable, although with smaller growth rates, well away from the light cone, typically as small k . Higher order interpolation has only modest impact on the non-resonant instability associated with the $m_z = -1$ alias, and almost no impact on that associated with the $m_z = 0$ alias. Fortunately, they can be reduced in growth rate by appropriate choices for ζ , such as those listed in Table 1, with $\zeta_x = \zeta_z =$

$$\frac{k k_z \frac{\Delta t}{2} \left(\sin^2 \left(k_z \frac{\Delta t}{2} \right) - \sin^2 \left(k \frac{\Delta t}{2} \right) \right) \csc \left(k_z \frac{\Delta t}{2} \right) \csc \left(k \frac{\Delta t}{2} \right)}{k_z \sin \left(k_z \frac{\Delta t}{2} \right) \cos \left(k \frac{\Delta t}{2} \right) - k \cos \left(k_z \frac{\Delta t}{2} \right) \sin \left(k \frac{\Delta t}{2} \right)} \quad (5)$$

when $k_z < \frac{\pi}{\Delta t} - k_x \frac{\Delta t}{4\pi}$ and 0 otherwise for option (c). Peak growth rates obtained using this strategy with cubic interpolation and the ten-pass digital filter given by

$$\cos^{16} \left(k_z \frac{\Delta z}{2} \right) \left(5 - 4 \cos^2 \left(k_z \frac{\Delta z}{2} \right) \right)^2 \cos^{16} \left(k_x \frac{\Delta x}{2} \right) \left(5 - 4 \cos^2 \left(k_x \frac{\Delta x}{2} \right) \right)^2 \quad (6)$$

and depicted in Fig. 7 of [5] are shown in Fig. 1. Growth rates for options (a) or (c) are sufficiently small that the numerical Cherenkov instability can safely be ignored in most applications when $v \Delta t/\Delta z < 1.3$. Growth rate curves were obtained by solving Eq.4 for the $m_z = +1, 0, -1$ aliases, and the simulation results using the WARP-PSATD PIC code[10]. In Figs. 1-5, $\gamma = 130$.

Option	Current Factors for Eq. 1
(a)	$\zeta_x = (k_x \Delta x/2) \cot(k_x \Delta x/2)$ $\zeta_z = (k_z \Delta z/2) \cot(k_z \Delta z/2)$
(b)	$\zeta_x = \zeta_z = 1$
(c)	$\zeta_x = \zeta_z$, as defined in Eq. 5

Table 1: Algorithm options used in Fig. 1 and elsewhere.

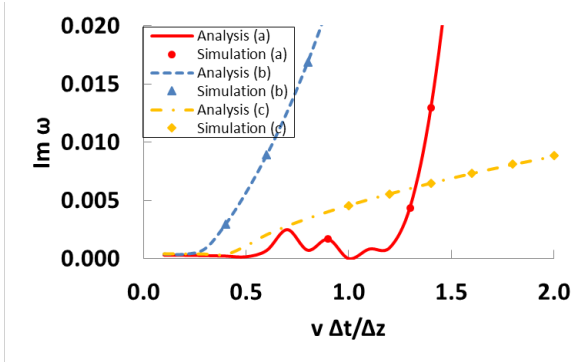


Figure 1: Maximum growth rates for options (a), (b), and (c) of Table 1 with cubic interpolation and the digital filter in Eq. 6. Markers represent corresponding simulation results.

3 High Gamma Results

The digital filter carried over from [5] and employed in obtaining Fig. 1 is quite aggressive, discarding about 70% of k-space in each dimension. (It was chosen to facilitate comparison with an earlier Finite Difference Time Domain (FDTD) numerical Cherenkov instability analysis [11] and with FDTD production simulations of Laser Plasma Acceleration [12, 13].) The effect of less aggressive filtering, in this case a sharp cutoff at $\alpha \min \left[\frac{\pi}{v \Delta t}, \frac{\pi}{\Delta z} \right]$ is illustrated in Fig. (2) for $\alpha = 1.0, 0.8, 0.6, 0.4$. The option (c) results from Fig. (1) are reproduced for comparison. Growth rates are scarcely affected by the choice of filtering for $v \Delta t / \Delta z > 1$, because option (c) is so effective at suppressing the $m_z = 0$ instability, which otherwise would dominate there. However, option (c) has only modest effect on the $m_z = -1$ instability, which typically dominates for $v \Delta t / \Delta z < 1$. As is evident from the figure, the choice of α matters greatly there, and $\alpha \lesssim 0.7$ is necessary to keep the numerical Cherenkov instability in check. Nonetheless, the sharp-cutoff digital filter at least doubles the proportion of usable k-space for $v \Delta t / \Delta z \approx 1$, compared to the filter in Eq. (6).

Incidentally, the maximum instability growth at larger $v \Delta t / \Delta z$ in Figs. (1) and (2) scales roughly

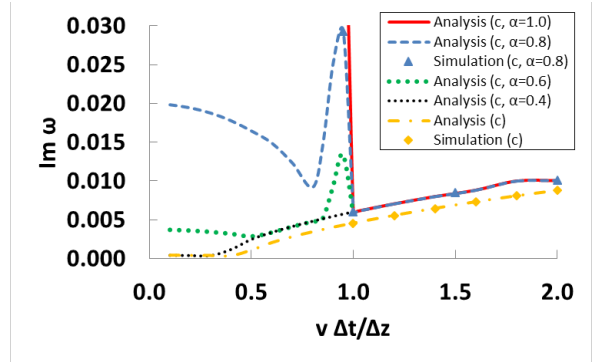


Figure 2: Maximum growth rates for option (c) of Table 1 with cubic interpolation and sharp-cutoff digital filter with threshold values $\alpha = 0.4, 0.6, 0.8, 1.0$. Markers represent corresponding simulation results.

as γ^{-1} but can be eliminated in part by making ζ_z for option (c) look more like ζ_z for option (a) at small k , for instance, by multiplying it by $\sin^{1/6}(k_z \Delta z / 2)$. (This odd expression was obtained by numerical trial and error.) Fig. 3 shows the effect of this factor for option (c) with $\alpha = 0.8$. The residual growth for $v \Delta t / \Delta z > 1$ is from higher order aliases and could be reduced further by using higher order interpolation, if desired.

The numerical Cherenkov instability can be viewed as arising from slight mismatches among the electric and magnetic fields due to finite differencing. Because peak growth rates tend to scale as the one-third power of the transverse force, even quite small errors are sufficient to produce the instabilities depicted in the preceding figures. Introducing the current scaling terms, ζ , in Eq. 1 helps to reduce these errors. An alternative, more direct approach is to rescale slightly the transverse fields as seen by the particles. For instance, choosing a multiplier for E_x ,

$$\frac{2 \frac{k}{k_z v} \sin^2 \left(\frac{k \Delta t}{2} \right) \sin \left(\frac{k_z v \Delta t}{2} \right) \cos \left(\frac{k_z v \Delta t}{2} \right)}{k \Delta t \sin^2 \left(\frac{k \Delta t}{2} \right) + (\sin(k \Delta t) - k \Delta t) \sin^2 \left(\frac{k_z v \Delta t}{2} \right)} \quad (7)$$

causes the term C_{2x} in Eq. 4 to vanish to order γ^{-2} at $\omega = k_z v$, thereby reducing the order of the highest order pole in the dispersion relation from 2 to 1 in

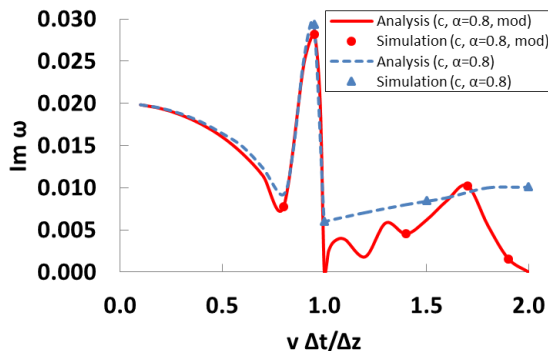


Figure 3: Maximum growth rates for option (c) of Table 1 with cubic interpolation and $\alpha = 0.8$ sharp-cutoff digital filter. The “mod” curve is obtained by modifying ζ_z as described in the text. Markers represent corresponding simulation results.

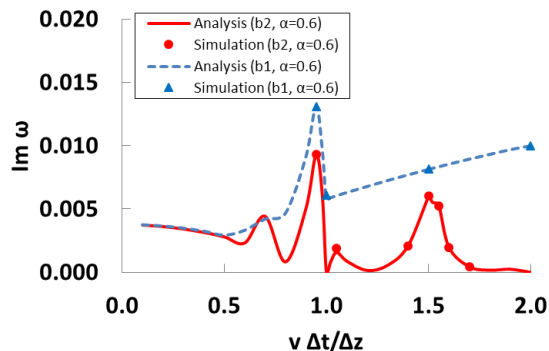


Figure 4: Maximum growth rates for field multiplier options (b1) and (b2) described in the text, cubic interpolation, $\zeta_z = \zeta_x = 1$, and $\alpha = 0.6$ sharp-cutoff digital filter. Markers represent corresponding simulation results.

the high- γ limit. The Fig. 4 curve labeled “b1” gives results for this multiplier, cubic interpolation, option (b) current factor, and $\alpha = 0.6$ sharp-cutoff digital filter. It is not surprising that the option (b1) curve strongly resembles the option (c), $\alpha = 0.6$ curve in Fig. 2, because option (c) also is designed to zero C_{2x} at $\omega = k_z v$ [5].

The second curve in Fig. 4, labeled “b2”, is based on an alternative pair of multipliers for E_x and B_y , respectively

$$\frac{k_z v \Delta t}{2} \cot\left(\frac{k_z v \Delta t}{2}\right), \frac{k \Delta t}{2} \cot\left(\frac{k \Delta t}{2}\right), \quad (8)$$

chosen to causes the term C_{3x} in Eq. 4 to vanish at $\omega = k_z v$, reducing the order of the highest order pole in the dispersion relation from 3 to 2. It is very effective at suppressing the numerical Cherenkov instability.

Note that an $\alpha = 0.6$ cutoff is used for options (b1) and (b2) to avoid a weak residual numerical Cherenkov instability that occurs at larger k_z and small k_x . This instability occasionally has been observed in the PSTD algorithm, described in Sec. 7 of [5], and in unpublished work by the first author on a version of PSATD employing vector potentials. It

can be described approximately by

$$C_0 + n \sum_{m_z} C_{2x} \csc^2 \left[(\omega - k'_z v) \frac{\Delta t}{2} \right] = 0 \quad (9)$$

for large γ . It appears to be triggered by the close proximity in k -space of the $m = 0$ numerical beam mode and one of the electromagnetic modes over a range of large k_z values when k_x is small. (No $m = 0$ instability occurs at $k_x = 0$, however.) Attempts apart from digital filtering to suppress this remaining $m = 0$ instability have been unsuccessful.

All the preceding methods for suppressing the numerical Cherenkov instability rely on digital filtering to curtail the $m_z = -1$ alias. At some cost in additional computation, it is straightforward to eliminate odd-numbered aliases entirely. For instance, one can simply double the number of cells in z while cutting Δz in half, then discard the upper half of k_z -space (suggested by Birdsall and Maron for electrostatic simulations [14]). This, coupled with cubic interpolation and option (c) modified, yields the maximum growth rate curve labeled “J : $\Delta z/2$, EB : $\Delta z/2$ ”, which is excellent. Of course, this approach approximately doubles the run time of a simulation. More economical is to compute currents as just described but compute fields and interpolate

them to the particles on the original, coarser mesh. This second approach increases the run time of the original simulation by only about 50% and produces modestly better stability properties besides. See the curve labeled “ $J : \Delta z/2, EB : \Delta z$ ”. Going one step further, one could compute the currents on the refined mesh as before but using splines based on a Δz rather than a $\Delta z/2$ unit cell. However, doing so achieves negligible improvement in run time or stability, and the curve labeled “ $J : \Delta z, EB : \Delta z$ ” is included only for completeness. For all three curves in this figure, Eq. 4 was solved for the $m_z = +2, 0, -2$ aliases.

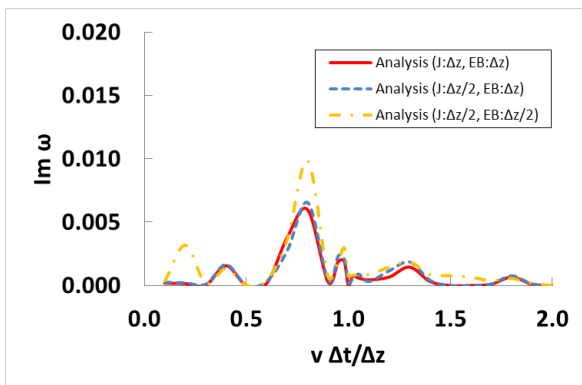


Figure 5: Maximum growth rates for odd- m_z elimination procedures described in the text, cubic interpolation, option (c) modified, and $\alpha = 0.8$ sharp-cutoff digital filter.

4 Low Gamma Results

Although the focus of this and the two preceding papers on suppressing the numerical Cherenkov instability [5, 11] is on highly relativistic beams, appropriate to Laser Plasma Accelerator simulations [13, 15], examining the scaling of numerical instabilities properties with γ is of interest both to validate the numerical dispersion relation of Eq. 4 over a range of beam energies and also to determine the robustness of proposed methods to suppress numerical instabilities. Fig 10 of [5] effectively substantiated the

dispersion relation itself, successfully comparing predicted instability growth rates with those measured in WARP for $\gamma = 130, 3.0, 1.4, 1.1$. Fig. 6 illustrates how peak growth rates vary with γ for one of the best instability suppression methods, option (c) modified with cubic interpolation and the $\alpha = 0.8$ sharp-cutoff digital filter. Instability growth rates, essentially independent of beam energy for $\gamma \gtrsim 10$, steadily increase for smaller beam energies due to the emergence of a well known, predominantly $m_z = -1$, non-relativistic, electrostatic numerical instability [6, 7]. The instability suppression method employed in Fig. 6 is, evidently, progressively less effective at lower beam energies, although it still is able to reduce peak growth by an order of magnitude for γ as small as 2.

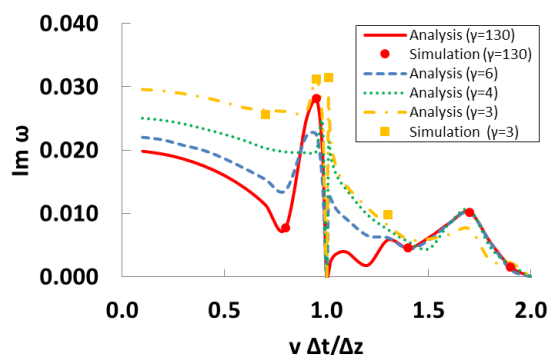


Figure 6: Maximum growth rates for $\gamma = 130, 6, 4, 3$, with cubic interpolation, option (c) modified, and $\alpha = 0.8$ sharp-cutoff digital filter. Markers represent corresponding simulation results.

Birdsall and Langdon years ago recommended “energy-conserving” algorithms [8, 14, 16, 17] for controlling the electrostatic numerical instability. Many variants are available. For the PSATD-Esirkepov algorithm the simple approach of offsetting E_z , the electric field aligned with the beam, by one-half cell in z works well, as illustrated in Fig. 7. The “Galerkin algorithm” described in [11], another energy-conserving algorithm, works not quite as well, not because it is ineffective against the electrostatic numerical instability but because it is less effective against the numerical Cherenkov instability [5]. Not

surprisingly, eliminating odd aliases, as described in the last section, also is quite effective at suppressing the numerical electrostatic instability.

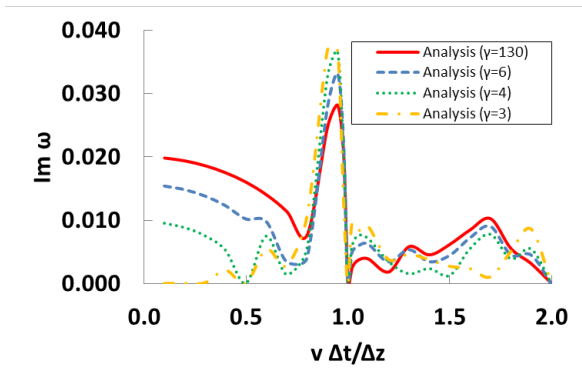


Figure 7: Maximum growth rates for $\gamma = 130, 6, 4, 3$, with E_z offset, cubic interpolation, option (c) modified, and $\alpha = 0.8$ sharp-cutoff digital filter.

The numerical instability suppression techniques described in this article are less effective against another instability, predicted in Problem 15-9a of [8], which occurs for $m_z = 0$ at very low γ . It satisfies the dispersion relation,

$$\sin^2\left(\omega \frac{\Delta t}{2}\right) - \sin^2\left(k \frac{\Delta t}{2}\right) - n (S^J)^2 \frac{\zeta_z \Delta t}{4k} \sin(k \Delta t) = 0, \quad (10)$$

obtained in a straightforward manner from Eq. 4 with $v = 0$ and $\zeta_z = \zeta_x$. (This dispersion relation is related to Eq. (59) in [5], which is valid for all γ but only at $k_x = 0$.) Eq. 10 has complex roots in typically very narrow bands in k -space located at just less than $k = l\pi/\Delta t$, l an integer. Fig. 8 shows that the maximum growth rate of this instability gradually decreases as the beam velocity increases. Growth of this instability vanishes for $v \gtrsim 0.8$, although growth rates from weaker instabilities remain visible in the figure. These calculations were performed for $m_z = +2, 0, -2$ aliases with cubic interpolation, $J : \Delta z$, $EB : \Delta z$ odd alias elimination, option (c) modified, and no digital filter. Without such

aggressive suppression of the numerical Cherenkov and electrostatic instabilities, the instability in question would not have been visible. Even so, all three instabilities have comparable maximum growth rates for $\Delta t/\Delta z = 1.2$.

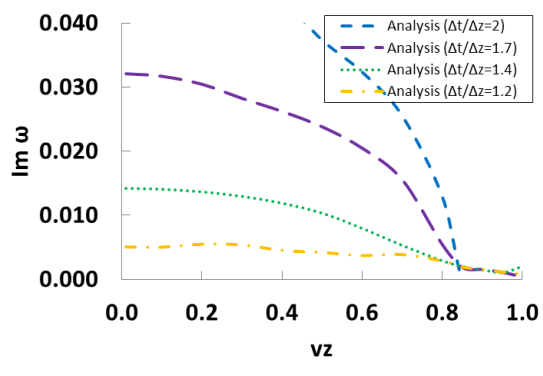


Figure 8: Maximum growth rates for $\Delta t/\Delta z = 2.0, 1.7, 1.4, 1.2$ with cubic interpolation, $J : \Delta z$, $EB : \Delta z$ odd alias elimination, option (c) modified, and no digital filter.

5 Conclusions

This paper introduces a variety of methods for suppressing the numerical Cherenkov instability in highly relativistic beam PSATD-Esirkepov PIC simulations complementing the methods introduced in [5]. Option (a) is both simple and highly effective for suppressing the numerical Cherenkov instability when $v \Delta t/\Delta z < 1.3$, at least for the parameters used in this paper. For larger values of $v \Delta t/\Delta z$, option (c) modified with $\alpha = 0.8$ seems best on balance. Option (b2) has modestly better stability properties but requires $\alpha = 0.6$ to avoid a new, not yet fully explained instability. The odd-alias elimination techniques also are highly effective, although at the cost of increased run time.

Numerical instability growth rates are nearly independent of beam energy for $\gamma \gtrsim 10$. At lower energies, the well known numerical electrostatic instability gradually increases in importance, becoming dom-

inant for $\gamma \lesssim 3$. Offsetting E_z by one-half cell in z is reasonably effective at controlling the electrostatic instability. The odd-alias elimination techniques seem highly effective here as well. Also to be considered at low energies is the numerical instability predicted by Birdsall and Langdon [8] for pseudo-spectral algorithms, which occurs at k an integer multiple of $\pi/\Delta t$. Although fairly weak and highly localized in k -space, this instability apparently cannot be suppressed except by strongly digitally filtering the tiny region of k -space in which it occurs.

A new instability unpredictably occurs in some instances in a small region of k -space located at large k_z and small k_x . Obtaining a better understanding of it is a priority of the first author.

Most of the results presented in this paper were obtained using Mathematica [9]. The authors intend to publish the Mathematica program used to produce the results in this article on a publicly accessible web site, <http://hifweb.lbl.gov/public/BLAST/Godfrey/>.

Acknowledgment

We thank David Grote for assistance with the code WARP. This work was supported in part by the Director, Office of Science, Office of High Energy Physics, U.S. Dept. of Energy under Contract No. DE-AC02-05CH11231 and the US-DOE SciDAC ComPASS collaboration, and used resources of the National Energy Research Scientific Computing Center.

References

- [1] I. Haber, R. Lee, H. Klein, and J. Boris, "Advances in electromagnetic simulation techniques," in *Proc. Sixth Conf. Num. Sim. Plasmas*, Berkeley, CA, 1973, pp. 46–48.
- [2] T. Esirkepov, "Exact charge conservation scheme for particle-in-cell simulation with an arbitrary form-factor," *Computer Physics Communications*, vol. 135, no. 2, pp. 144–153, 2001.
- [3] J.-L. Vay, I. Haber, and B. B. Godfrey, "A domain decomposition method for pseudo-spectral electromagnetic simulations of plasmas," *Journal of Computational Physics*, vol. 243, pp. 260–268, 2013.
- [4] B. B. Godfrey, "Numerical cherenkov instabilities in electromagnetic particle codes," *Journal of Computational Physics*, vol. 15, no. 4, pp. 504–521, 1974.
- [5] B. B. Godfrey, J.-L. Vay, and I. Haber, "Numerical stability analysis of the pseudo-spectral analytical time-domain pic algorithm," 2013.
- [6] A. B. Langdon, "Nonphysical modifications to oscillations, fluctuations, and collisions due to space-time differencing," in *Proceedings of the fourth conference on numerical simulation of plasmas*, 1970, pp. 467–495.
- [7] H. Okuda, "Nonphysical instabilities in plasma simulation due to small debye length," in *Proceedings of the fourth conference on numerical simulation of plasmas*, 1970, pp. 511–525.
- [8] C. K. Birdsall and A. B. Langdon, *Plasma physics via computer simulation*. Taylor & Francis, 2005.
- [9] Mathematica, version nine. Wolfram Research Inc. [Online]. Available: <http://www.wolfram.com/mathematica/>
- [10] D. Grote, A. Friedman, J.-L. Vay, and I. Haber, "The warp code: modeling high intensity ion beams," in *AIP Conference Proceedings*, no. 749, 2005 2005, pp. 55–58.
- [11] B. B. Godfrey and J.-L. Vay, "Numerical stability of relativistic beam multidimensional pic simulations employing the esirkepov algorithm," *Journal of Computational Physics*, vol. 248, pp. 33–46, 2013.
- [12] J.-L. Vay, C. G. R. Geddes, E. Cormier-Michel, and D. P. Grote, "Numerical methods for instability mitigation in the modeling of laser wake-field accelerators in a lorentz-boosted frame,"

Journal of Computational Physics, vol. 230, no. 15, pp. 5908–5929, Jul. 2011.

- [13] J.-L. Vay, C. G. R. Geddes, E. Esarey, C. B. Schroeder, W. P. Leemans, E. Cormier-Michel, and D. P. Grote, “Modeling of 10 gev-1 tev laser-plasma accelerators using lorentz boosted simulations,” *Physics of Plasmas*, vol. 18, 2011.
- [14] C. K. Birdsall and N. Maron, “Plasma self-heating and saturation due to numerical instabilities,” *Journal of Computational Physics*, vol. 36, pp. 1–19, 1980.
- [15] J.-L. Vay, C. G. R. Geddes, E. Cormier-Michel, and D. P. Grote, “Effects of hyperbolic rotation in minkowski space on the modeling of plasma accelerators in a lorentz boosted frame,” *Physics of Plasmas*, vol. 18, p. 030701, 2011.
- [16] H. R. Lewis, “Variational algorithms for numerical simulation of collisionless plasma with point particles including electromagnetic interactions,” *Journal of Computational Physics*, vol. 10, no. 3, pp. 400–419, 1972.
- [17] A. B. Langdon, “Energy-conserving plasma simulation algorithms,” *Journal of Computational Physics*, vol. 12, no. 2, pp. 247–268, 1973.